Preparation of PAN/lycopene-TiO$_2$ nanocomposite membrane for azo dye degradation

Devi Baskar[a], Gobi Nallathambi[a,*], Arun Karthick Selvam[b], P. Senthil Kumar[c,*]

[a]*Department of Textile Technology, Anna University, Chennai – 600 025, India, emails: gobsnn@gmail.com (G. Nallathambi), famidevi@gmail.com (D. Baskar)*
[b]*Feynman Nano Laboratory, Department of Biomedical Engineering, Sri Sivasubramaniya Nadar College of Engineering, Rajiv Gandhi Salai (OMR), Kalavakkam – 603 110, Chennai, India, email: arunkarthicks@ssn.edu.in*
[c]*Department of Chemical Engineering, Sri Sivasubramaniya Nadar College of Engineering, Rajiv Gandhi Salai (OMR), Kalavakkam – 603 110, Chennai, India, email: senthilkumarp@ssn.edu.in*

ABSTRACT

In this study, lycopene TiO$_2$ nanoparticles complex incorporated electrospun polyacrylonitrile (PAN) nanocomposite membrane was prepared for azo dye degradation by electrospinning process. The material was characterized by using scanning electron microscopy and Fourier transform infrared spectroscopy. Membrane surface wettability, membrane performance and Congo red dye degradation were studied and the degraded products were identified by gas chromatography mass spectroscopy. From the results, it was found that the 30% of lycopene TiO$_2$ nanoparticles complex incorporated electrospun PAN nanocomposite membranes showed better surface wettability, pure water flux and antifouling property than the other membranes. These membranes also showed higher dye degradation efficiency than the other membranes due to better distribution and lesser agglomeration of lycopene TiO$_2$ nanoparticles complex. Among the nanocomposite membranes with 30% of lycopene TiO$_2$ nanoparticles complex, the membrane which was electrospun for 5 h showed higher membrane surface wettability, optimum pure water flux, higher recovery ratio and higher percentage of congo red dye degradation. Hence this membrane can be effectively used as a photocatalytic membrane to degrade azo dyes under visible light irradiation.

Keywords: Lycopene TiO$_2$ nanoparticles complex; Polyacrylonitrile; Nanocomposite membrane; Dye degradation; Electrospinning

1. Introduction

Membrane technology is gaining interest among the researchers for water treatment. Among the fabrication techniques, electrospinning is the technique widely used to prepare nanocomposite membranes. In the electrospinning process, an electric field is applied to the polymer solution, which induces a charge on the polymer surface. The charge repulsion induces a force, which is directly opposite to the surface tension. As the electric field is increased, the Taylor cone is formed and when the electric field reaches a critical value, a charged jet is ejected from the Taylor cone and deposited on the collector [1]. Thus formed electrospun nanofibres have excellent properties such as large surface area, small pores, high porosity, ease of separation and reusability [2,3]. These nanofibres are embedded with nanoparticles in order to produce functional electrospun nanofibres, which are good candidates for water filtration and treatment because of their low density and interconnected open pore structure [4–8]. Electrospun nanofibres are used for dye degradation by incorporating the photocatalytic material.

* Corresponding authors.

Im et al. [9] prepared electrospun polyacrylonitrile (PAN)-based nanofibre webs containing TiO_2 and the webs were evaluated for the photodecomposition of dye rhodamine B under UV light. They found that floating of electrospun PAN-based fibre webs containing titania improved the irradiation efficiency [9]. Polyacrylonitrile (PAN) is the polymer used as the base material because of their advantages such as easy availability, easy to spin and high tensile strength [6]. Titanium dioxide is the most widely used semiconductor material for photocatalysis because of their advantages such as chemically stable, low cost, high efficiency, nontoxic and biocompatible [10–12]. The limitations of TiO_2 nanoparticles are as follows: active only under UV light, high rate of electron–hole recombination and difficult to recover after photocatalytic process in chemical wastewater treatment methods [11,13]. To overcome these two disadvantages of TiO_2, the TiO_2 material was sensitized with dye molecule and incorporated into an electrospun polymeric nanocomposite membrane. Dye sensitization is the method used in the preparation of solar cells, which converts light energy into electrical energy. The process in which a photoanode is adsorbed with a dye molecule to harvest the sunlight is known as dye-sensitized solar cells. These dye molecules are natural pigments such as carotenoids, anthocyanins, tannins, chlorophylls, cyanins, flavonoids, etc., which were widely used to sensitize TiO_2 materials [14,15]. Lycopene is a natural pigment, which gives orange red color to plants, vegetables and fruits. Ezeh et al. [16] extracted the lycopene from tomato and used to sensitize the TiO_2 and Shinde et al. [14] have reported the extraction of lycopene from carrot and coated it over the zirconium oxide to enhance its photocatalytic property. Among the dyes, azo dyes are the largest class of synthetic chemicals used widely in textile, leather, food, printing, plastic and pharmaceutical industries. These azo dyes are characterized by N=N attached to the two aromatic rings, which are toxic to the environment. Hence it is vital to degrade the residual azo dyes that are present in the wastewater streams into non-toxic metabolites [17,18].

In our previous work, the preparation and characterization of lycopene–TiO_2 nanoparticles complex by simple process [10] was reported. In this present work, lycopene–TiO_2 nanoparticles complex embedded electrospun polyacrylonitrile (PAN) nanocomposite membrane was fabricated, there is no literature for the use of lycopene–TiO_2 nanoparticles complex as a photocatalyst for dye degradation and the incorporation of lycopene–TiO_2 nanoparticles complex material into the electrospun PAN nanocomposite membrane. Hence this lycopene–TiO_2 nanoparticles complex incorporated electrospun PAN nanocomposite membrane was studied for the dye degradation of Congo red under visible light source.

2. Experimental setup

2.1. Materials

Polyacrylonitrile $(C_3H_3N)_n$ (PAN) with molecular weight of 150,000 g/mol and bovine serum albumin (BSA) with molecular weight of 66 kDa was obtained from Sigma-Aldrich, St. Louis, USA. The solvent dimethyl formamide (DMF) and the dye Congo red was purchased from SRL ltd.

India. Lycopene–TiO_2 nanoparticles complex (LTC) was used as prepared. All chemicals were used as received without any further treatment.

2.2. Preparation of LTC

Liquid–liquid extraction method was used to extract lycopene from tomato fruit and purified using column chromatography [19]. Thus purified lycopene was used to synthesize titanium dioxide nanoparticles. Titanium tetrabutoxide was used as a precursor to synthesize TiO_2 and lycopene acts as reducing agent as well as ligand to form lycopene–TiO_2 nanoparticles complex. To the precursor solution, lycopene was added and stirred well for 24 h. Then the solution was centrifuged at 4,000 rpm for 60 min and the pellets were collected, dried in hot air oven at 75°C and kept in a furnace for 3 h at 450°C [10]. Thus the lycopene TiO_2 nanoparticles complex was synthesized.

2.3. Fabrication of lycopene-TiO_2 nanoparticles complex incorporated electrospun PAN nanocomposite membrane (LTC-E-PAN)

The concentration of the polymer PAN was kept as constant, which is 12%. The electrospinning time and the LTC percentage were varied to prepare the nanocomposite membrane. Table 1 shows the parameters used to prepare electrospun PAN/lycopene-TiO_2 nanocomposite membrane.

The polymer solution was prepared by dissolving PAN (12%) in DMF. Once PAN dissolved completely, LTC was added and stirred further to obtain homogeneous solution. Now the LTC-incorporated PAN solution was ready for electrospinning. The electrospinning parameters are maintained as follows: flow rate at 0.5 mL/h, voltage applied at the tip was 18 kV, the tip to collector distance was 15 cm. Thus the nine samples of electrospun PAN/lycopene–TiO_2 nanocomposite membranes were prepared.

2.4. Characterization

The morphology of the membranes was analyzed by using scanning electron microscope (HITACHI S-3400 SEM) and the ImageJ software was used to measure the nanofibre diameter of the prepared LTC-incorporated electrospun PAN nanocomposite membranes (E-PAN-LTC).

Table 1
Parameters to prepare LTC-incorporated electrospun PAN nanocomposite membranes

Sample name	LTC percentage (%)	Electrospinning time (h)
E1	20	3
E2	30	
E3	40	
E4	20	4
E5	30	
E6	40	
E7	20	5
E8	30	
E9	40	

Fourier transform infrared spectroscopy (FTIR) (JASCO 6600 type A) equipped with attenuated total reflectance was used to study the functional groups of the membrane materials. The FTIR spectrum was recorded for sample E9 because the chemical components are same for all the prepared membranes.

To study the water uptake and porosity of the membranes, membrane samples were cut into 1 cm × 1 cm size and soaked in distilled water for 24 h. After 24 h, the excess water on the membrane was removed and wet weight of the membrane was calculated by using the following formula:

$$\%\text{Water uptake} = \left(\frac{W_w - W_d}{W_w} \right) \times 100 \tag{1}$$

where W_w = wet weight of the membrane and W_d = dry weight of the membrane.

The gravimetric method was used to calculate the porosity of the membrane using the formula:

$$\% \text{ Porosity} = \left(\frac{W_w - W_d}{A \times l \times \text{dw}} \right) \times 100 \tag{2}$$

where A = area of the membrane (m²); l = thickness of the membrane (m); dw = density of water (g cm⁻³).

2.5. Pure water flux

Membrane performance was evaluated by measuring pure water flux and antifouling property. A dead end filtration set up was used to evaluate the membrane performance. Pure water flux is calculated by the following formula:

$$J_{\text{WF1}} = \frac{Q}{A\Delta T} \tag{3}$$

where Q = permeated pure water (L); A = effective membrane area (m²); ΔT = testing duration (h).

2.6. Dye adsorption study

Membrane surface fouling was evaluated by Congo red adsorption on the membranes. The membranes were cut into 1 cm × 1 cm size with known weight and soaked in distilled water for 24 h and then kept in dye solution under gentle shaking for 6 h. After 6 h of shaking, the UV-visible spectroscopy was recorded. The amount of dye adsorbed was calculated by using the following equation:

$$R = \left(1 - \frac{C_R}{C_0} \right) \times 100 \tag{4}$$

where C_R = remaining concentration and C_0 = initial concentration of dye solution.

2.7. Antifouling property

The antifouling property of the membranes was studied by using BSA protein of concentration 1,000 ppm as model foulant. Pure water flux (J_{WF1}) was measured at 250 mm Hg pressure using dead end filtration set up. Then the membrane was washed thoroughly with distilled water and tested with BSA protein solution under same conditions. The protein flux (J_p) was measured. Again the pure water flux (J_{WF2}) was measured under similar conditions after the washing process.

The fouling resistance of the membrane was evaluated with flux recovery ratio by the following equation:

$$\text{FRR}\left(\%\right) = \left(\frac{J_{\text{WF2}}}{J_{\text{WF1}}} \right) \times 100 \tag{5}$$

Overall the total fouling ratio (R_t), reversible fouling (R_r) and irreversible fouling (R_{ir}) were calculated by the following equation:

$$R_t\left(\%\right) = \left(1 - \frac{J_P}{J_{\text{WF1}}} \right) \times 100 \tag{6}$$

$$R_r\left(\%\right) = \left(\frac{J_{\text{WF2}} - J_P}{J_{\text{WF1}}} \right) \times 100 \tag{7}$$

$$R_{\text{ir}}\left(\%\right) = \left(\frac{J_{\text{WF1}} - J_{\text{WF2}}}{J_{\text{WF1}}} \right) \times 100 \tag{8}$$

2.8. Dye degradation

The dye degradation of the membranes was studied by using a simple in-house photocatalytic membrane reactor set up design. The set up consists of three main parts, which are millipore motor, visible light source and filtration unit that holds membrane. 100 mL of Congo red dye solution (30 mg) was filled in the upper jar of the filtration unit and the set up was closed. The visible light source and the motor were switched on and the dye solution passes through the membrane. The dye solution was collected at every 10 min interval and the absorbance values are recorded using UV-visible spectroscopy. The percentage of dye degradation was determined by the following equation:

$$\text{Dye degradation}\left(\%\right) = \left(\frac{C_0 - C_t}{C_0} \right) \times 100 \tag{9}$$

where C_0 and C_t are the initial and final concentration of the dye solution.

GC-MS (Shimadzu QP 5000 equipment, Japan) was taken for the membrane, which showed higher dye degradation in order to find the products of the degraded dye. The test process conditions were ionization voltage was 70 eV, gas chromatography was conducted in temperature programming mode with a Restek column (0.25 mm × 30 mm, XTI-5). The initial column temperature was 40°C for 4 min, which was linearly increased at a rate of 10°C/min to 270°C and held at 4 min. The injection port temperature was 275°C and GC-MS interface was maintained at 300°C. The carrier gas, flow rate and the run time were helium gas, 1 mL/min and 30 min respectively.

The compounds were identified based on the mass spectra and the NIST library stored in the computer software (version 1.10 beta Shimadzu, Japan) of the GC-MS.

3. Results and discussion

The synthesized lycopene TiO_2 nanoparticles complex (LTC) was spherical in shape, size ranges from 80 to 250 nm and contains highly crystalline anatase phase of TiO_2 [10].

3.1. Scanning electron microscope

Fig. 1 shows the SEM micrographs of LTC-incorporated electrospun PAN nanocomposite membrane samples E1, E2 and E3. The average fibre diameter of the LTC-E-PAN nanocomposite membranes E1, E2 and E3 were measured by using ImageJ software and the values are 359, 190 and 338 nm. As the percentage of LTC increases from 20% to 30%, the fibre diameter decreases from 359 to 190 nm due to the increased solution conductivity and decreased viscosity, hence the reduced fibre diameter was observed. Further increase in the LTC percentage, increases the nanofibre diameter because of the agglomeration of the LTC, which reduces the solution conductivity and also increased the viscosity [20]. The histogram clearly indicated that the E1 nanocomposite membrane has more number of nanofibres diameter in the range of 350 to 400 nm, E2 nanocomposite membrane in the range of 180 to 200 nm and E3 nanocomposite membrane in the range of 320 to 340 nm.

3.2. Fourier transform infrared spectroscopy

The FTIR spectrum of LTC-incorporated electrospun PAN nanocomposite membrane (Fig. 2) shows that the characteristic absorption peak of PAN was found at 2,243 cm^{-1} corresponds to the nitrile functional group (−C≡N). The absorption peaks obtained at 1,072 cm^{-1} indicate the presence of C−O stretch; 1,044 cm^{-1} indicates the presence Ti−O−C stretch and 535 cm^{-1} corresponds to the Ti−O stretch vibration; these are the characteristic peaks of LTC. The absorption peaks at 1,732 and 1,230 cm^{-1} corresponds to the C=O and C−N stretching functional groups of the solvent DMF and the peaks at 872 cm^{-1} indicates the CH stretching of lycopene. The others peaks from 2,930–2,870 cm^{-1}; 1,460–1,450 cm^{-1}; 1,380–1,360 cm^{-1} and 1,363 cm^{-1} indicates the CH_2 functional groups of lycopene and PAN, whereas peaks at 2,938, 2,869 and 1,449 cm^{-1} correspond to the CH group of lycopene and PAN [10,21,22].

3.3. Water uptake and porosity

Water uptake and porosity are the two important parameters, which describe the hydrophilic nature of the membranes, which are tabulated in Table 2. The table presents the GSM, thickness, water uptake and porosity of LTC-incorporated electrospun PAN nanocomposite membranes. Membranes with 20% of LTC and 40% of LTC have better water uptake and porosity whereas membranes with 30% of LTC showed higher water uptake and porosity. The water uptake and porosity of the membranes may be attributed to the fact that the LTC incorporated
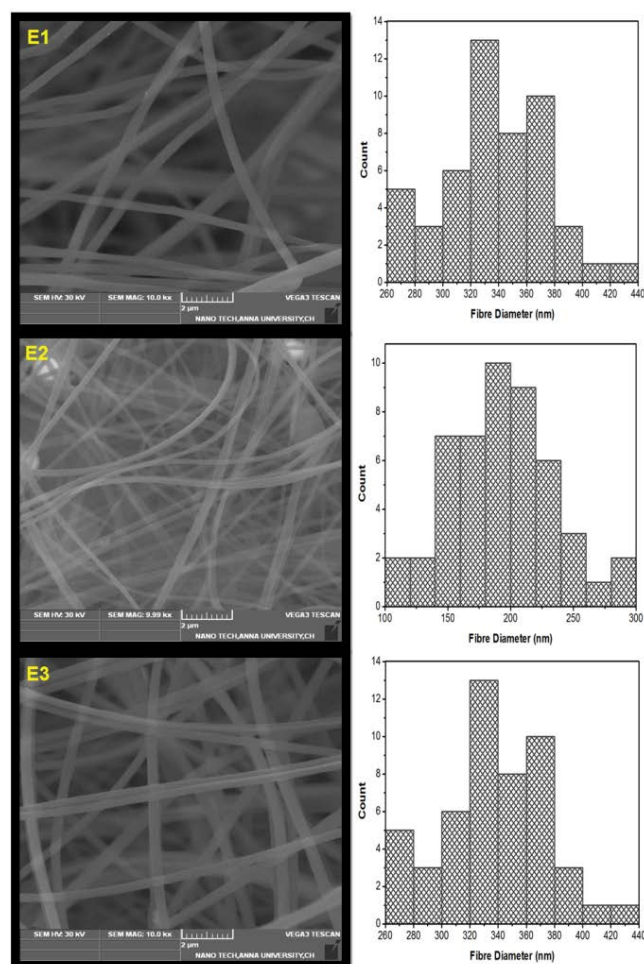

Fig. 1. SEM micrographs of LTC-incorporated electrospun PAN nanocomposite membranes.

into the PAN nanofibres agglomerates and block the pores of the nanofibres, which led to the decrease in the porosity of the membranes. Fig. 3 shows the water uptake and porosity percentages of LTC-incorporated electrospun PAN nanocomposite membranes.

3.4. Pure water flux

Pure water flux (J_{WF1}) was measured for all the membranes (Fig. 4) and it was found that the 20% and 40% of LTC embedded in the PAN nanocomposite membranes showed higher pure water flux than the 30% LTC; this phenomenon depends on the fibre diameter of the membrane. Incorporation of LTC in the PAN nanofibres has an effect on the fibre diameter, which was already discussed in the section 3.1. The diameter of the nanofibre is directly proportional to the pore size [23]. Larger diameter of the fibres leads to larger pore size; this in turn increases the pure water flux.

3.5. Antifouling property

Antifouling property of the membranes was studied by using BSA protein flux study (Fig. 4). Incorporation of

Table 2
GSM, thickness, water uptake and porosity of LTC-incorporated electrospun PAN nanocomposite membranes

S. No	Sample name	LTC percentage (%)	Electrospinning time (h)	GSM (g/m²)	Thickness (mm)	Water uptake (%)	Porosity (%)
1	E1	20	3	9	0.092	67	20
2	E2	30		6	0.046	85	72
3	E3	40		8	0.083	68	21
4	E4	20	4	10	0.098	69	22
5	E5	30		7	0.061	88	87
6	E6	40		10	0.091	72	29
7	E7	20	5	13	0.104	72	33
8	E8	30		9	0.079	89	95
9	E9	40		12	0.099	76	37
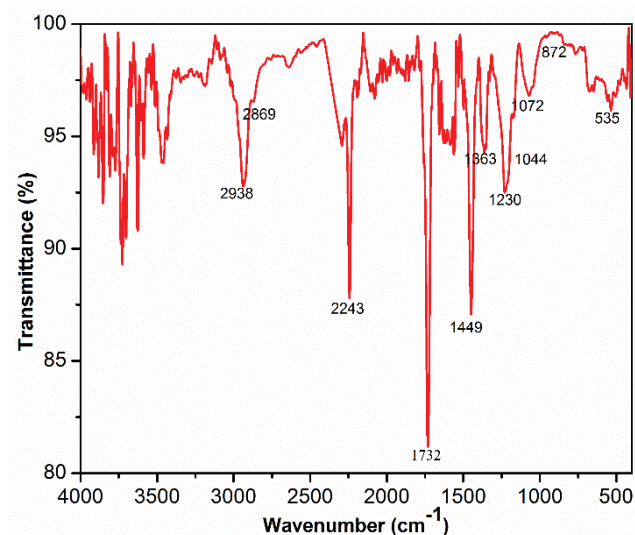
Fig. 2. FTIR spectrum of LTC-incorporated electrospun PAN nanocomposite membrane.

Fig. 3. Water uptake and porosity of LTC-incorporated electrospun PAN nanocomposite membranes.

LTC improves the hydrophilic nature of the membranes, which leads to the nonspecific protein adsorption because of the high surface hydration. It was observed that the initial pure water flux (J_{WF1}) for all the LTC-incorporated electrospun PAN nanocomposite membranes were higher when compared with the flux (protein flux [J_P]) observed during the antifouling study (Fig. 4). This is due to the binding of BSA protein molecules to the membrane surfaces, thus causes fouling. 20% and 40% of LTC embedded PAN nanocomposite membranes were found to have less protein flux than the initial pure water flux, which implies the amount of BSA protein deposited on the membrane surface is higher whereas 30% LTC-incorporated membranes too showed similar results but the decline in the flux was less. Among the 30% of LTC-incorporated electrospun PAN nanocomposite membranes, E8 showed the lesser flux decline since the lesser amount of BSA binding on the surface of the membrane. Again the pure water flux (J_{WF2}) was measured after washing the membranes, there was an increase in the flux for all the membranes. Fig. 5 represents th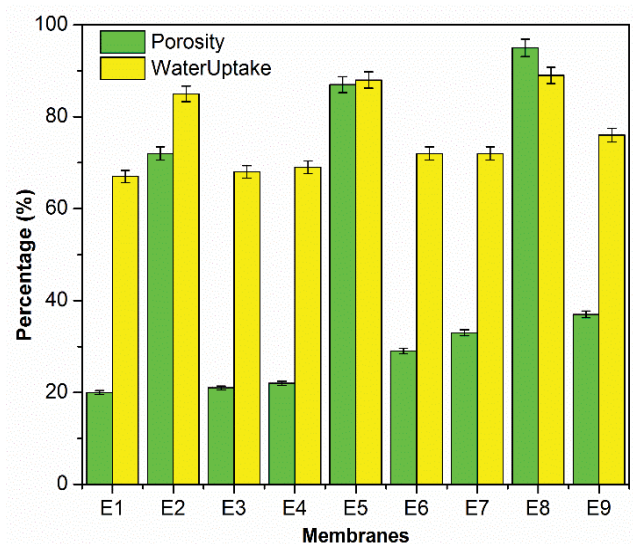e flux recovery; irreversible and reversible flux for LTC-incorporated electrospun PAN nanocomposite membrane. From the graph, the higher flux recovery was observed for the membranes incorporated with 30% of LTC due to the lesser amount of BSA protein binding. Among the 30% of LTC-incorporated electrospun PAN nanocomposite membranes, E8 membrane showed higher flux recovery of 68% after washing process. Hence they are regarded as more antifouling and the fouling is considered as reversible fouling. All the membranes were found to have higher irreversible fouling than the reversible fouling, except membrane E8. These results could be ascribed to the addition of LTC in the PAN nanocomposite membrane, which lead to the increased membrane hydrophilicity [24].

3.6. Adsorption study

Membrane fouling can also be caused by the adsorption of molecules on the membrane surface. Hence the adsorption of Congo red dye was studied for all the membranes (Fig. 6), 20% and 40% of LTC-incorporated electrospun PAN nanocomposite membranes showed higher adsorption
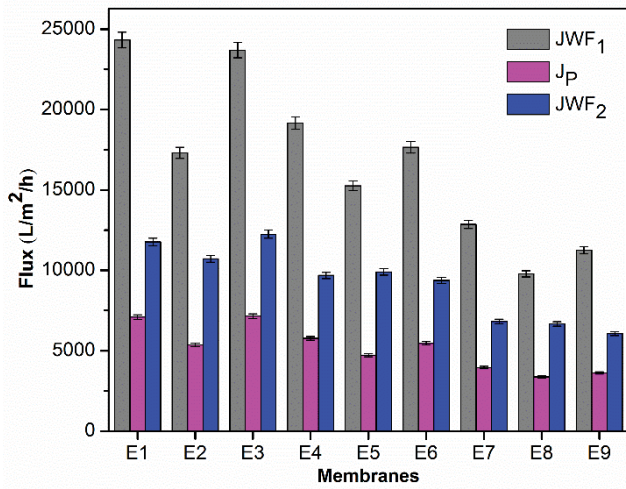
Fig. 4. Antifouling property of LTC-incorporated electrospun PAN nanocomposite membranes.
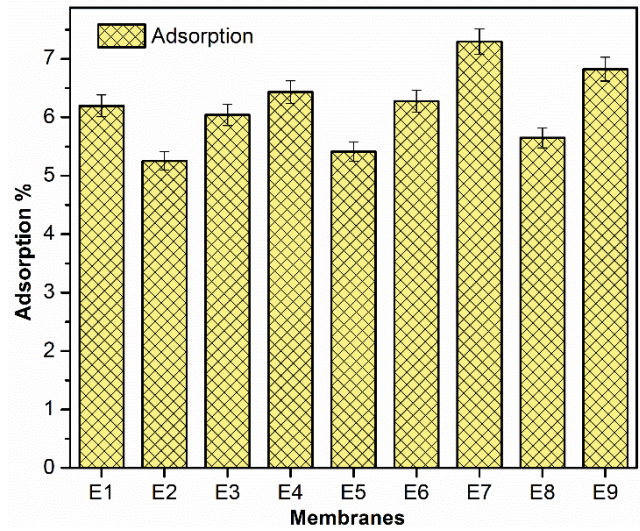

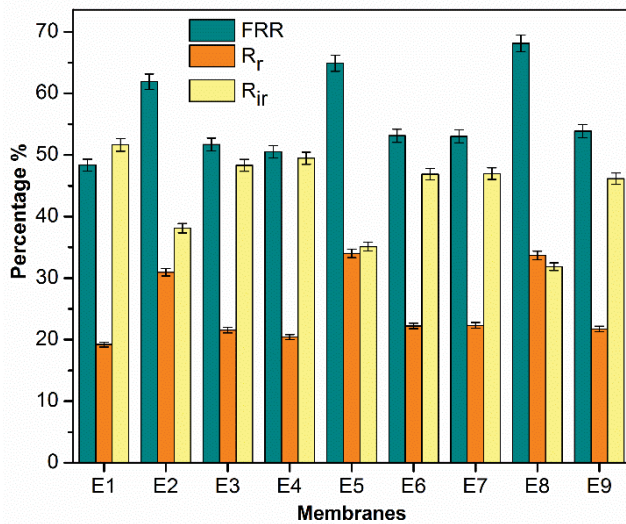Fig. 6. Congo red dye adsorption of LTC-incorporated electrospun PAN nanocomposite membranes.

Fig. 5. Flux recovery, irreversible and reversible flux for LTC-incorporated electrospun PAN nanocomposite membranes.

Fig. 7. Congo red dye degradation of LTC-incorporated electrospun PAN nanocomposite membranes.

percentage due to the adsorption of higher amount of congo red on the surface of the membranes whereas 30% of LTC-incorporated electrospun PAN nanocomposite membranes showed lesser adsorption percentage. The reason for the lesser amount of Congo red adsorption on the membrane surface was due to the increased membrane hydrophilicity [24]. Thus the 30% of LTC-incorporated electrospun PAN nanocomposite membranes have better productivity than the 20% and 40% of LTC-incorporated electrospun PAN nanocomposite membrane.

3.7. Congo red dye degradation and kinetics

Fig. 7 represents the Congo red dye degradation percentage profile of LTC-incorporated electrospun PAN nanocomposite membranes. It was observed that the 30% of LTC-incorporated electrospun PAN nanocomposite
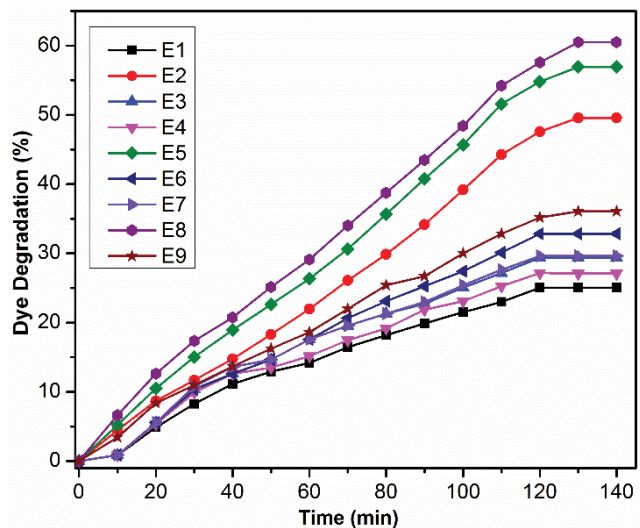
membranes showed higher congo red dye degradation than the 20% and 40% of LTC-incorporated electrospun PAN nanocomposite membranes. Among the 30% of LTC-incorporated electrospun PAN nanocomposite membranes, E8 have higher congo red dye degradation of 60% in 140 min, which is due to the presence of LTC with lesser agglomeration. This slight lower dye degradation percentage (60%) may be attributed due to the following experimental conditions such as room temperature, neutral pH and visible light source. Similar results were reported by Im et al. [25] in which they have prepared PAN/TiO$_2$ nanofibres for photocatalytic degradation (Rhodamine B). TiO$_2$ containing mat suspended on the dye solution has higher dye removal of 60% comparing with immersed one, whereas the immersed mat showed 20% of color removal after 48 h and also the dye degradation of PAN/TiO$_2$ was studied under UV light.

Several literatures reported the dye degradation fitted to simple pseudo-first order kinetics [26,27]. Hence Congo red dye degradation data were fitted by the simple pseudo-first order kinetics with respect to dye concentration. The equation used for the kinetic study is as follows:

$$\ln\left[\frac{C_t}{C_0}\right] = -K_{(obs)}t \tag{10}$$

The rate constant (K_{obs}) and R^2 values are presented in Table 3. All the data were well fitted to pseudo-first order kinetics ($R^2 > 0.9$) and all the 30% LTC-incorporated electrospun PAN nanocomposite membranes showed higher Congo red dye degradation as well as higher rate constant.

The Congo red dye degradation products were identified by using GC-MS and the proposed mechanism was depicted in Fig. 8. The GC-MS spectra of the degraded products of Congo red dye are shown in Table 4.

From the results, the proposed mechanism initially involves that the sulfonate group in the Congo red dye ionize out an anion [28]. In the next step, the azo bond cleaves

and gives rise to an unknown compound and the biphenyl-4,4′-diamine. Biphenyl-4,4′-diamine undergo deamination to form biphenyl (m/z – 154), whereas unknown compound undergo deamination and desulfonation to form naphthalene

Table 3
Rate constant and R^2 values of LTC-incorporated electrospun PAN nanocomposite membranes

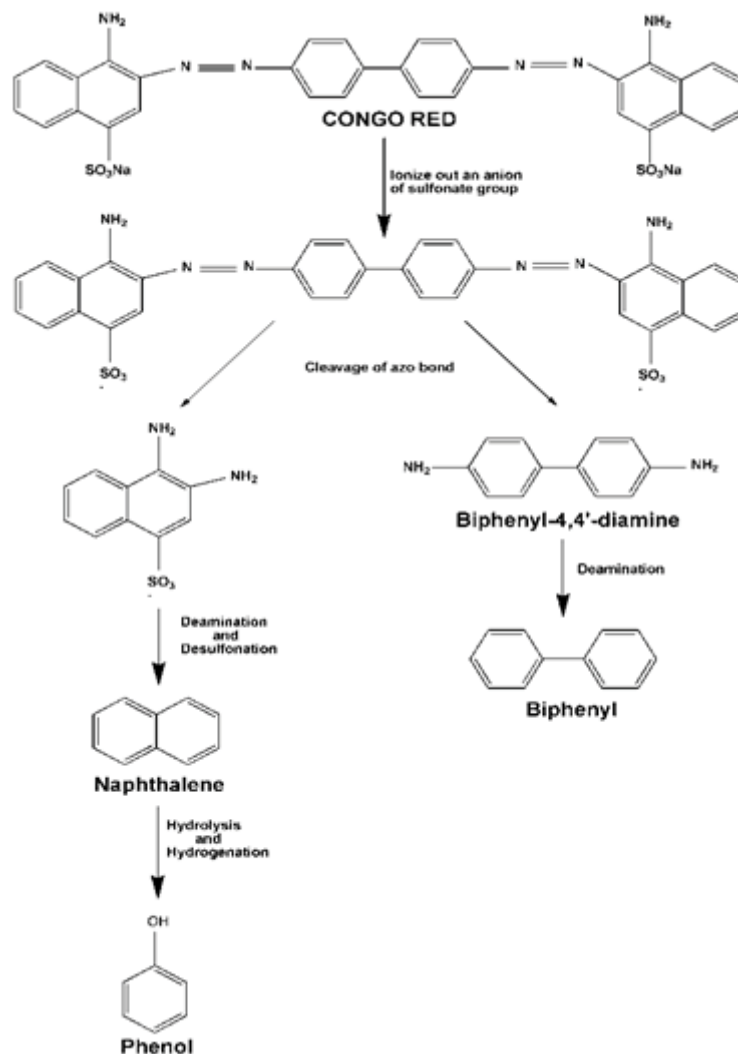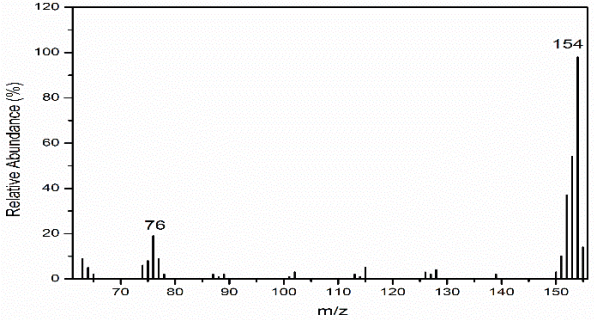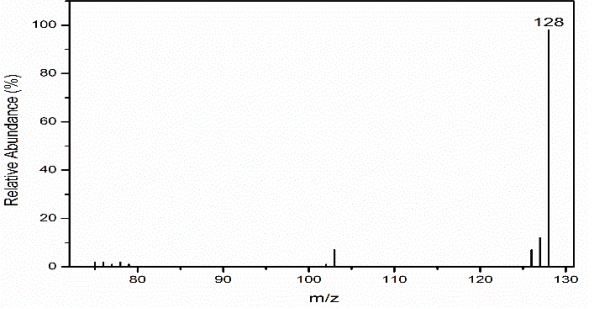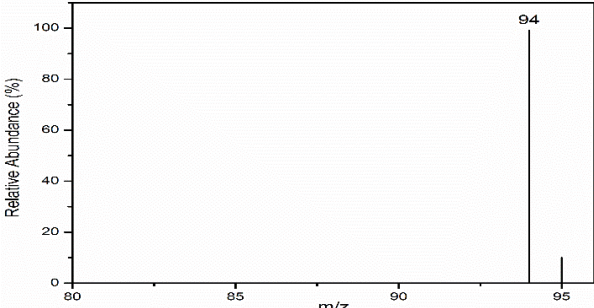| S. No	Membranes name	K_{obs}	R^2
1	E1	0.05241	0.96875
2	E2	0.1318	0.98018
3	E3	0.06347	0.96948
4	E4	0.0573	0.96708
5	E5	0.16095	0.98221
6	E6	0.07534	0.98229
7	E7	0.06391	0.96734
8	E8	0.17289	0.98524
9	E9	0.08076	0.99109

Fig. 8. Proposed mechanism of Congo red dye degradation by LTC-incorporated electrospun PAN nanocomposite membrane.

Table 4
GC-MS spectra of the degraded products of Congo red dye degradation by LTC-incorporated electrospun PAN nanocomposite membranes

Name of the product	Molecular weight	Mass spectrum (m/z)
Biphenyl	154	
Naphthalene	128	
Phenol	94	

(m/z – 128). Further, this naphthalene reduces to phenol (m/z – 94) by hydrolysis and hydrogenation reaction [29].

4. Conclusion

Lycopene TiO$_2$ nanoparticles complex incorporated electrospun PAN nanocomposite membrane was fabricated. It was found that the 30% of LTC-incorporated electrospun PAN nanocomposite membranes showed better results than the 20% and 40% of LTC-incorporated electrospun PAN nanocomposite membranes. This is attributed to the incorporation of LTC, which lead to the decreased fibre diameter, increased water uptake and porosity. Larger diameter leads to larger pores, which in turn increases the pure water flux. Among the 30% of LTC-incorporated electrospun PAN nanocomposite membranes, the membrane, which was electrospun for 5 h (E8), showed lower pure water flux due to its smaller fibre diameter. The antifouling properties were studied by using BSA protein molecule, which binds to the membrane surface and causes fouling. The amount of BSA bound to membrane surface was less for 30% of LTC-incorporated electrospun PAN nanocomposite membranes. E8 membrane showed highest flux recovery of 68% after the simple washing step. Adsorption of the Congo red dye shows the lesser adsorption on the membrane surface due to its increased hydrophilicity. And also the E8 membrane achieved maximum congo red dye degradation of 60% under visible light and the degraded products were identified as biphenyl, naphthalene and phenol. Among the LTC-incorporated electrospun PAN nanocomposite membranes, E8 membrane can be effectively used as a photocatalytic membrane without compromising the membrane properties.

Acknowledgment

References

[1] J. Doshi, D.H. Reneker, Electrospinning Process and Applications of Electrospun Fibers, Conference Record of the 1993 IEEE Industry Applications Conference Twenty-Eighth IAS Annual Meeting, IEEE, 1993, pp. 1698–1703.

[2] J. Hou, J. Yun, H. Byun, Fabrication and characterization of modified graphene oxide/PAN hybrid nanofibre membrane, Membranes, 9 (2019) 122.

[3] Z. Yuan, X. Cheng, L. Zhong, R. Wu, Y. Zheng, Preparation, characterization and performance of an electrospun carbon nanofiber mat applied in hexavalent chromium removal from aqueous solution, J. Environ. Sci., 77 (2019) 75–84.

[4] D. Baskar, A.K Selvam, M. Ganesan, G. Nallathambi, Mechanism of nanofibres on removal of water pollutants - a review, Indian J. Chem. Technol., 25 (2018) 451–458.

[5] S.A. Karthick, N. Gobi, Nano silver incorporated electrospun polyacrylonitrile nanofibres and spun bonded polypropylene composite for aerosol filtration, J. Ind. Text., 46 (2017) 1342–1361.

[6] Q. Liu, Y. Zheng, L. Zhong, X. Cheng, Removal of tetracycline from aqueous solution by a Fe_3O_4 incorporated PAN electrospun nanofiber mat, J. Environ. Sci., 28 (2015) 29–36.

[7] A.K. Selvam, G. Nallathambi, Polyacrylonitrile/silver nanoparticle electrospun nanocomposite matrix for bacterial filtration, Fiber Polym., 16 (2015) 1327–1335.

[8] A.K Selvam, G. Nallathambi, Mesoporous $MgAl_2O_4$ and $MgTiO_3$ nanoparticles modified polyacrylonitrile nanofibres for 2-chloroethyl ethyl sulfide degradation, Fibers Polym., 16 (2015) 2121–2129.

[9] J.S. Im, M.I. Kim, Y.S. Lee, Preparation of PAN-based electrospun nanofibre webs containing TiO_2 for photocatalytic degradation, Mater. Lett., 62 (2008) 3652–3655.

[10] D. Baskar, G. Nallathambi, Dual functional property of lycopene as a reducing agent to synthesis TiO_2 nanoparticles and as a ligand to form lycopene-TiO_2 nanoparticles complex, Mater. Lett., 209 (2017) 303–306.

[11] D. Chakrabortty, S.S. Gupta, Photo-catalytic decolourisation of toxic dye with N-doped titania: a case study with acid blue 25, J. Environ. Sci., 25 (2013) 1034–1043.

[12] Z. Chen, J. Zhao, X. Yang, Q. Ye, K. Huang, C. Hou, Y. Li, Fabrication of TiO_2/WO_3 composite nanofibers by electrospinning and photocatalytic performance of the resultant fabrics, Ind. Eng. Chem. Res., 55 (2016) 80–85.

[13] V. Buscio, S. Brosillon, J. Mendret, M. Crespi, C. Gutiérrez-Bouzán, Photocatalytic membrane reactor for the removal of CI disperse red 73, Materials, 8 (2015) 3633–3647.

[14] D.R. Shinde, P.S. Tambade, K.M. Gadave, K.S. Pawar, M. Naushad, H.M. Pathan, Dye-sensitised solar cells with a naturally occurring pigment lycopene as a photosensitiser for zirconium dioxide: an experimental and theoretical study, J. Mater. Sci. Mater. Electron., 28 (2017) 11311–11316.

[15] E. Yamazaki, M. Murayama, N. Nishikawa, N. Hashimoto, M. Shoyama, O. Kurita, Utilization of natural carotenoids as photosensitizers for dye-sensitized solar cells, Sol. Energy, 81 (2007) 512–516.

[16] M.I. Ezeh, O.F. Eyekpegha, O.L. Mayiko, Fabrication of Dye Sensitized Solar Cell Using ITO/TiO$_2$/ZNO/lycopene (Tomato) Dye Sensitized, Proceedings of the 1st African International Conference/Workshop on Applications of Nanotechnology to Energy, Health and Environment, 2014, pp. 47–54.

[17] S. Priyaragini, S. Veena, D. Swetha, L. Karthik, G. Kumar, K.B. Rao, Evaluating the effectiveness of marine actinobacterial extract and its mediated titanium dioxide nanoparticles in the degradation of azo dyes, J. Environ. Sci., 26 (2014) 775–782.

[18] G. Zhang, S. Zhang, Quantitative structure-activity relationship in the photodegradation of azo dyes, J. Environ. Sci., 90 (2020) 41–50.

[19] S. Metkar, S. Saptarshi, A. Kadam, Studies on extraction, isolation and applications of lycopene, Indo Am. J. Pharm. Res., 4 (2014) 1462–1474.

[20] A. Razzaz, S. Ghorban, L. Hosayni, M. Irani, M. Aliabadi, Chitosan nanofibres functionalized by TiO_2 nanoparticles for the removal of heavy metal ions, J. Taiwan Inst. Chem. Eng., 58 (2016) 333–343.

[21] O. Eren, N. Ucar, A. Onen, N. Kizildag, I. Karacan, Synergistic effect of polyaniline, nanosilver, and carbon nanotube mixtures on the structure and properties of polyacrylonitrile composite nanofibre, J. Compos. Mater., 50 (2016) 2073–2086.

[22] S. Tas, O. Kaynan, E. Ozden-Yenigun, K. Nijmeijer, Poly-acrylonitrile (PAN)/crown ether composite nanofibres for the selective adsorption of cations, RSC Adv., 6 (2016) 3608–3616.

[23] R. Roche, F. Yalcinkaya, Electrospun polyacrylonitrile nano-composite membranes for point-of-use water and air cleaning, Chem. Open, 8 (2019) 97–103.

[24] B.P. Tripathi, N.C. Dubey, R. Subair, S. Choudhury, M. Stamm, Enhanced hydrophilic and antifouling polyacrylonitrile membrane with polydopamine modified silica nanoparticles, RSC Adv., 6 (2016) 4448–4457.

[25] J.S. Im, M.I. Kim, Y.S. Lee, Preparation of PAN-based electrospun nanofiber webs containing TiO_2 for photocatalytic degradation, Mater. Lett., 62 (2008) 3652–3655.

[26] R.A. Damodar, S.J. You, H.H. Chou, Study the self cleaning, antibacterial and photocatalytic properties of TiO_2 entrapped PVDF membranes, J. Hazard. Mater., 172 (2009) 1321–1328.

[27] R.A. Damodar, S.J. You, Performance of an integrated membrane photocatalytic reactor for the removal of reactive black 5, Sep. Purif. Technol., 71 (2010) 44–49.

[28] Y.J. Zhang, L. Kang, L.C. Liu, In: F. Pacheco-Torgal, J. Labrincha, C. Leonelli, A. Palomo, P. Chindaprasit, Handbook of Alkali-Activated Cements, Mortars and Concretes, Woodhead Publishing, UK, 2015, pp. 729–775.

[29] H. Lade, S. Govindwar, D. Paul, Mineralization and detoxification of the carcinogenic azo dye Congo red and real textile effluent by a polyurethane foam immobilized microbial consortium in an upflow column bioreactor, Int. J. Environ. Res. Public Health, 12 (2015) 6894–6918.